

On the Robustness of Next Generation GNSS Phase-only Real-Time Kinematic Positioning

Lennard HUISMAN¹, Peter J.G. TEUNISSEN^{1,2}, Dennis ODIJK¹

Key words: Phase-only RTK, GNSS, multipath

SUMMARY

The coming years will show a proliferation of Global and Regional Navigation Satellite Systems (GNSS). This promise of a broader multi-frequency, multi-constellation "system of systems" has the potential to enable a wide range of demanding applications for high-accuracy users. For such applications, successful GNSS ambiguity resolution, which is the process of resolving the unknown cycle ambiguities of double-difference (DD) carrier-phase data as integers, is essential. The sole purpose of ambiguity resolution is to use the integer ambiguity constraints as a means of improving significantly on the precision of the remaining model parameters, such as baseline coordinates and/or atmospheric delays. Ambiguity resolution applies to a great variety of current and future GNSS models. These models differ greatly in complexity and diversity. They range from single-baseline models used for real-time kinematic (RTK) positioning to multi-baseline models used as a tool for studying geodynamic phenomena. The increase in signals, frequencies and satellites has enormous potential for increasing the robustness of GNSS models.

In this contribution we study and analyze the robustness of multi-frequency GNSS models for phase-only RTK processing. Our attention is restricted to the short baseline application, neglecting the influence of atmospheric errors, but it is stressed that the phase-only RTK model is also applicable for longer baselines. We use the ambiguity success-rate as our measure for phase only performance. Using experimental results we show that the phase-only RTK model is more robust in case of multipath than the traditional phase+code RTK model.

On the Robustness of Next Generation GNSS Phase-only Real-Time Kinematic Positioning

Lennard HUISMAN¹, Peter J.G. TEUNISSEN^{1,2}, Dennis ODIJK¹

1. INTRODUCTION

Global Navigation Satellite System (GNSS) ambiguity resolution is the process of resolving the unknown cycle ambiguities of double difference (DD) carrier phase data as integers. The sole purpose of ambiguity resolution is to use the integer ambiguity constraints as a means of improving significantly on the precision of the remaining model parameters, such as baseline coordinates and/or atmospheric delays.

Ambiguity resolution applies to a great variety of current and future GNSS models. These models may differ greatly in complexity and diversity. They range from single-baseline models used for kinematic positioning to multi-baseline models used as a tool for studying geodynamic phenomena. The models may or may not have the relative receiver-satellite geometry included. They may also be discriminated as to whether the slave receiver(s) are stationary or in motion. When in motion, one solves for one or more trajectories, since with the receiver-satellite geometry included, one will have new coordinate unknowns for each epoch. One may also discriminate between the models as to whether or not the differential atmospheric delays are included as unknowns. In the case of sufficiently short baselines they are usually excluded. Apart from the current Global Positioning System (GPS) models, carrier phase ambiguity resolution also applies to the future modernized GPS and the future European Galileo GNSS. An overview of GNSS models, together with their applications in surveying, navigation, geodesy and geophysics, can be found in textbooks such as [*Parkinson and Spilker*, 1996], [*Strang and Borre*, 1997], [*Teunissen and Kleusberg*, 1998], [*Leick*, 2004], [*Misra and Enge*, 2006], [*Hofmann-Wellenhof et al.*, 2008].

In this contribution we study and analyze the robustness of current and modernized GPS models for phase-only RTK processing (see table 1). The methodology developed is generally applicable and can therefore also be applied to other GNSSs. Short baselines without atmospheric delays are considered. The phase-only GPS model for short-baselines is full of rank providing a minimum of two epochs are used.

carrier signal	notation	frequency (MHz)	wave length (cm)
L1	ϕ_1	$154 \times 10.23 = 1575.420$	$\lambda_1 = 19.03$
L2	ϕ_2	$120 \times 10.23 = 1227.600$	$\lambda_2 = 24.42$
L5	ϕ_3	$115 \times 10.23 = 1176.450$	$\lambda_3 = 25.48$

Table 1: Modernized GPS signals

We study the impact of the third GPS frequency, the number of satellites and the measurement precision on phase-only processing. We use the ambiguity success-rate as our measure for phase only performance. The potential advantage of using carrier phase-only data is that ambiguity resolution will be freed from any biasing effects that the code data may bring (e.g. code multipath). Using experimental results we show that the phase-only RTK model is more robust in case of multipath than the traditional phase+code RTK model.

2. INTEGER AMBIGUITY RESOLUTION

2.1 The GNSS model

In principle all GNSS models can be cast in the following frame of linear(ized) observation equations,

$$E(y) = Aa + Bb \quad , \quad D(y) = Q_{yy} \quad , \quad a \in Z^n \quad , \quad b \in R^p \quad (1)$$

where y is the given GNSS data vector of order m , a and b are the unknown parameter vectors respectively of order n and p , E and D are the expectation and dispersion operator, respectively, A and B are the given design matrices that link y to a and b , and where Q_{yy} is the given variance matrix of y . The data vector y may consist of the 'observed minus computed' single-, dual- or triple frequency double-difference (DD) phase and/or pseudorange (code) observations accumulated over all observation epochs. The entries of vector a are then the DD carrier phase ambiguities, expressed in units of cycles rather than range. They are known to be *integers*, $a \in Z^n$. The entries of the vector b will consist of the remaining unknown parameters, such as for instance baseline components (coordinates) and possibly atmospheric delay parameters. They are known to be real-valued, $b \in R^p$.

When using the least-squares (LS) principle, the GNSS model can be solved by means of the minimization problem

$$\min_{a,b} \|y - Aa - Bb\|_{Q_{yy}}^2 \quad , \quad a \in Z^n \quad , \quad b \in R^p \quad (2)$$

with $\| \cdot \|_{Q_{yy}}^2 = (\cdot)^T Q_{yy}^{-1} (\cdot)$

The solution of this *integer* LS problem can be obtained in the following three steps,

$$\left\{ \begin{array}{l} (i) \quad \begin{bmatrix} \hat{a} \\ \hat{b} \end{bmatrix} \quad , \quad \begin{bmatrix} Q_{\hat{a}\hat{a}} & Q_{\hat{a}\hat{b}} \\ Q_{\hat{b}\hat{a}} & Q_{\hat{b}\hat{b}} \end{bmatrix} \\ (ii) \quad \tilde{a} = \arg \min_{a \in Z^n} \| \hat{a} - a \|_{Q_{\hat{a}\hat{a}}}^2 \\ (iii) \quad \tilde{b} = \hat{b} - Q_{\hat{b}\hat{a}} Q_{\hat{a}\hat{a}}^{-1} (\hat{a} - \tilde{a}) \end{array} \right. \quad (3)$$

In the first step one simply discards the integer constraints $a \in Z^n$ on the ambiguities and performs a standard LS adjustment. As a result one obtains the (real-valued) LS estimates \hat{a} and \hat{b} , together with their variance matrix. The solution of this first step is referred to as the 'float' solution. In the second step the 'float' ambiguity estimate \hat{a} is used to compute the corresponding integer LS ambiguity estimate \tilde{a} . Once these integer ambiguities are computed, they are used in the third step to finally correct the 'float' estimate of b , so as to obtain the 'fixed' estimate \tilde{b} .

The above integer LS solution can be computed efficiently with the popular LAMBDA (Least-squares AMBiguity Decorrelation Adjustment) method, see e.g. [Teunissen, 1995], [de Jonge and Tiberius, 1996].

2.2 The ambiguity success-rate

In order to evaluate the expected performance of ambiguity resolution, we need the probability mass function (PMF) of the estimated ambiguities \tilde{a} . If we denote the probability density function (PDF) of \hat{a} as $p_{\hat{a}}(x)$, the PMF of \tilde{a} follows as

$$P(\tilde{a} = z) = \int_{S_z} p_{\hat{a}}(x) dx \quad , \quad z \in Z^n \quad (4)$$

with the regions of integration given as $S_z = \{x \in R^n \mid \|x - z\|_{Q_{\hat{a}}}^2 \leq \|x - u\|_{Q_{\hat{a}}}^2, \forall u \in Z^n\}$ and the PDF - in case of Gaussian distributed data - given as

$$p_{\hat{a}}(x) = \frac{1}{\sqrt{\det(Q_{\hat{a}})} (2\pi)^{\frac{1}{2}n}} \exp\left\{-\frac{1}{2} \|x - a\|_{Q_{\hat{a}}}^2\right\} \quad (5)$$

The probability of *correct* integer ambiguity estimation, $P(\tilde{a} = a)$, is of particular interest. It describes the expected success-rate of GNSS ambiguity resolution. Different ways of evaluating the least-squares success-rate have been given in [Teunissen, 1998]. In the present contribution we make use of the very easy-to-compute lower bound

$$P(\tilde{a} = a) \geq \prod_{i=1}^n \left(2\Phi\left(\frac{1}{2\sigma_{i|I}}\right) - 1\right) \quad (6)$$

with

$$\Phi(x) = \int_{-\infty}^x \frac{1}{\sqrt{2\pi}} \exp\left\{-\frac{1}{2}v^2\right\} dv$$

and where the $\sigma_{i|I}$, $i=1, \dots, n$, denote the sequential conditional standard deviations of the decorrelated ambiguities. This lower bound was introduced in [Teunissen, 1999] and it is presently the sharpest lower bound available for (6), see e.g. [Thomson, 2000], [Verhagen, 2003].

3. SHORT BASELINE PHASE-ONLY AMBIGUITY RESOLUTION

3.1 The short baseline phase-only GPS model

In this section we present the expected performance of phase-only ambiguity resolution for short baselines, using different measurement scenarios. In case of sufficiently short baselines, the unknown ionospheric and tropospheric delays may be assumed absent. The short-baseline, phase+code, multiple frequency model reads,

$$\begin{aligned} p_j(i) &= G(i)b \\ \phi_j(i) &= \lambda_j a_j + G(i)b \end{aligned} \quad (7)$$

with $p_j(i)$ and $\phi_j(i)$, ($j=1,2,3$), respectively the vector of DD code observations and the vector of DD carrier phase data on frequency f_j . a_j denotes the unknown time invariant

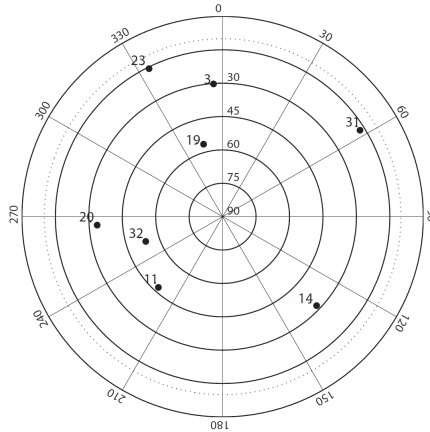


Figure 1: Skyplot for selected time span

vector of the integer ambiguities of frequency f_j and b the vector of unknown stationary baseline components. The matrix $G(i)$ captures the relative receiver-satellite geometry at epoch i , λ_j for $j=1,2,3$ denote the known wavelengths of GPS.

The phase-only model lacks the code observations $p_j(i)$:

$$\phi_j(i) = \lambda_j a_j + G(i)b \quad (8)$$

The model is of full-rank from the outset, provided at least two epochs of data are used. Hence, no special precautions have to be taken to eliminate rank defects.

For the standard deviation of observations used in our computations we use an elevation dependent weighting model, which reads,

$$\sigma_{\phi_i}^s = \sigma_{\phi_i} (1 + 10 \exp\{-\frac{\delta^s}{10}\}) \quad (9)$$

where the elevation dependency is described by the ratio $\frac{\sigma_{\phi_i}^s}{\sigma_{\phi_i}}$ and δ^s the elevation of satellite s in degrees.

3.2 Short baseline phase-only success-rates

In the following sections we will look at the dependency of the phase-only GPS-model on the number of frequencies, the number of satellites, the measurement precision and the time interval between measurement epochs. The ambiguity success-rate will be our measure for the performance of the phase-only GPS-model in different scenarios. The ambiguity success-rate will be computed using the lower-bound given in (6). From (6) it is clear that the success-rates depend on the variance-covariance matrix of the decorrelated ambiguities. For a known position and satellite constellation we can perform design computations, without observations, to obtain the expected variance covariance matrix of the decorrelated ambiguities, therefore the expected lower bound for the ambiguity success-rates can be computed without observations.

In the design computations it is assumed that the phase ambiguities remain constant during the complete time span, in this case we can take full advantage of the changing satellite-

receiver geometry. The computations have been performed for a location in Perth, Western Australia, for a dual-epoch observation. The chosen start time for the computations is the first epoch of the experimental data set used in section 3.3. Figure 1 shows a skyplot of the visible satellites above 10 degrees elevation during the time span with this constellation.

3.2.1 Single frequency, Dual frequency and Triple frequency

In this section the influence of the number of satellites and the number of frequencies on the success-rates is investigated. The constellation in figure 1 shows 8 satellites, for the computations with less satellites each time the satellite at the lowest elevation has been removed, so for example in the computations with 6 satellites, satellites with PRN 23 and 31 were removed from the design scenario. Table 2 shows the success-rates for the different scenarios.

Frequencies	Success-rate 4 satellites	Success-rate 5 satellites	Success-rate 6 satellites	Success-rate 7 satellites	Success-rate 8 satellites
L1	0.0000	0.0000	0.0002	0.0036	0.1602
L1/L2	0.2159	0.7564	0.9993	1.0000	1.0000
L1/L5	0.2500	0.8382	0.9999	1.0000	1.0000
L2/L5	0.1554	0.9227	1.0000	1.0000	1.0000
L1/L2/L5	0.9850	1.0000	1.0000	1.0000	1.0000

Table 2: The phase-only dual-epoch success-rate for different frequencies with 1 second time interval and $\sigma_{\phi_i} = 1 \text{ mm}$

The table shows that, as can be expected, the more satellites and the more frequencies used the better the success-rates. From the first row it is clear that single-frequency phase-only successful ambiguity resolution is unlikely for short time spans. The success-rate of dual-frequency and triple-frequency are close to one from 6 satellites tracked. The L1/L5 linear combination, which is interesting from a GPS/Galileo combined perspective as Galileo will also broadcast signals on these frequencies, is always outperforming the L1/L2 dual frequency scenario for this constellation.

3.2.2 Measurement precision

The measurement precision has an influence on the success-rates, because it directly influences the precision of the estimated float ambiguities. The value chosen for the coefficient σ_{ϕ_i} in the elevation dependent weighting model of (9) in the previous section is 1 millimeter for all phase observations. The influence of this coefficient on the a-priori standard deviation of the observables versus elevation is shown in figure 2 and the influence on the success-rates is shown in table 3.

$\sigma_{\phi_i} [mm]$	Success-rate with 6 satellites	Success-rate with 7 satellites
1	0.9993	1.0000
2	0.6976	0.9649
3	0.1878	0.5940

Table 3: The phase-only dual-epoch success-rate for different measurement precision dual-frequency (L1/L2) observations with 1 second time interval

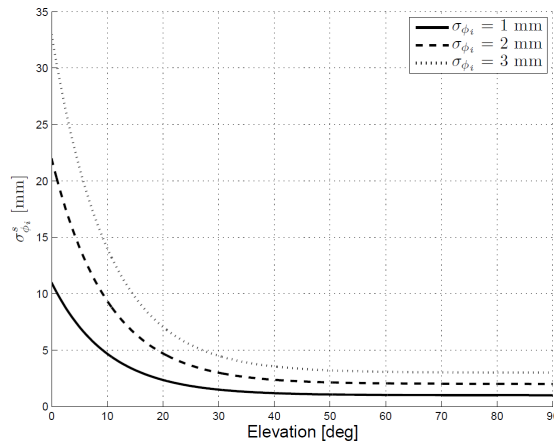


Figure 2: Elevation dependent weighting function for different values of coefficient σ_{ϕ_i}

The influence of the measurement precision is evident from table 3. It shows the sensitivity of the design computations for not only the number of satellites but also the chosen measurement precision. The measurement precision of currently available GPS-RTK equipment is close to or better than 1 millimeter. For example the Sokkia equipment used in the experiment in section 3.3 has a specified measurement precision of 0.5 mm for *L1* and 1 mm for *L2*.

A value for the standard deviation of 1 mm in zenith direction when an elevation dependent weighting model is used is also recommended in scientific software such as the Bernese GPS software [Dach *et al.*, 2007]. The results show that dual-epoch phase-only ambiguity resolution should therefore be possible with current surveying grade receivers and 7 satellites in view.

3.2.3 Time interval

Although with 6 or more satellites and a state of the art measurement precision the dual-frequency, dual-epoch phase-only success-rates are close to one for a time interval of 1 second, a larger time interval means that the satellite-receiver geometry has changed more, which will make the phase-only model stronger. Figure 3 shows the influence of larger time spans for the single frequency success-rates. The figure shows two lines, one line where all available data, with a time span of 1 second, is used and one line where the first and last epoch, so only two epochs, of the time interval are used for the computation of the success-rates. It is clear from figure 3 that it is not only the redundancy that makes single frequency phase-only ambiguity resolution possible, but also the change in geometry has a strong effect in improving the success-rates. We are only investigating (modernized) GPS at the moment, but it can be expected that more satellite systems will also have a large impact on the single frequency phase-only ambiguity resolution as this will have an impact on both the geometry and the redundancy.

3.3 Phase-only fixed baselines in case of multipath

In the previous section we have shown that dual-epoch phase-only ambiguity resolution is possible. In this section we will show the effect of multipath on dual epoch ambiguity resolution and the baseline coordinates in the phase-only and the traditional phase and code

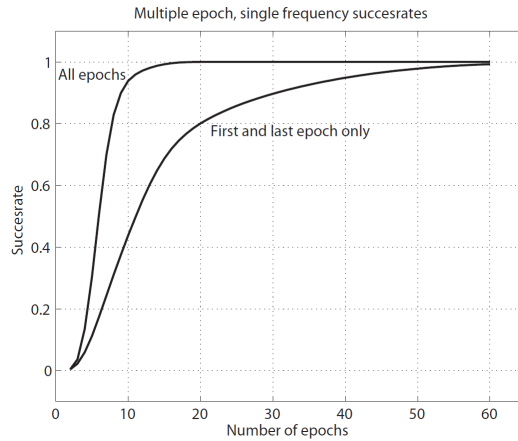


Figure 3: Phase-only success-rates using all epochs (top) and using only the first and last epoch (bottom) versus time interval, $\sigma_{\phi_i} = 1 \text{ mm}$

GPS-model. The data used in this section is that of a 100 meter baseline and was collected using Sokkia GSR2700ISX receivers. Figure 4 shows the satellite constellation for the selected measurement interval of 2000 seconds.

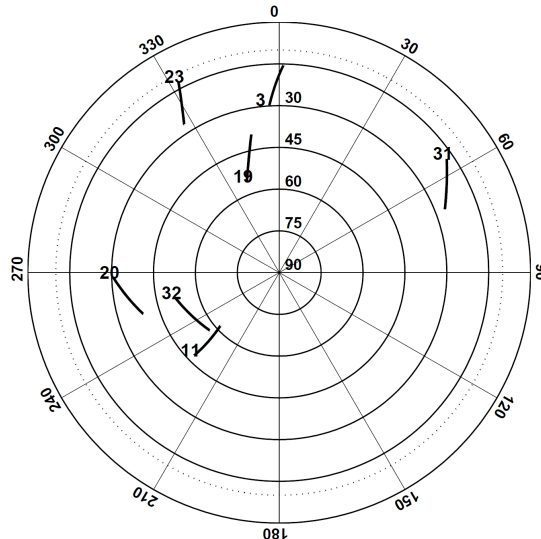


Figure 4: Skyplot for the experimental dataset

Compared to the scenario of the design computations in section 3.2 there is one satellite less (PRN14), which gives 7 satellites that were continuously tracked by both receivers.

3.3.1 Multipath simulation

Since the data was collected in a multipath free environment multipath has to be simulated on the observables. In the following sections it is assumed that there is a vertical reflecting surface present that reflects the satellite signals. Figure 5 gives a geometric interpretation of a vertical reflecting surface.

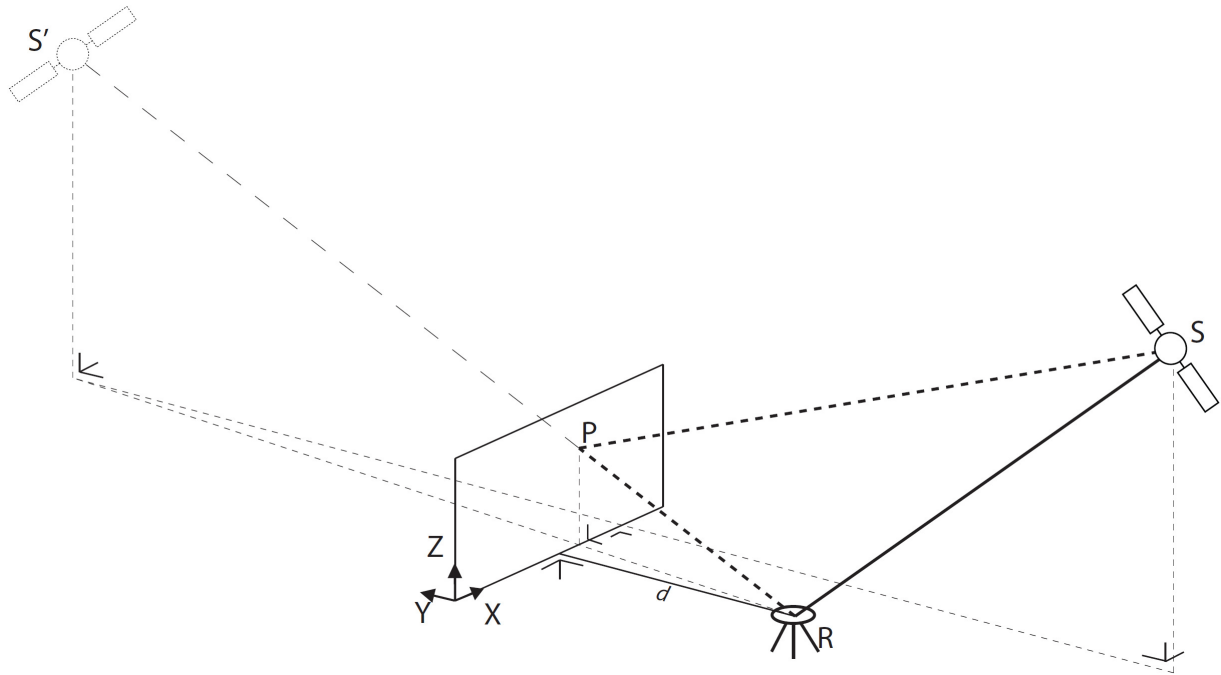


Figure 5: The length of the direct path and the delayed in case of a vertical reflector

There is a direct signal SR from satellite S to receiver R and a reflected signal $SP-PR$, where P is the point of incidence. The length of the reflected path can easily be computed as $S'R$ where S' is the image of S in the coordinate system with its origin in the lower left corner of the plane.

The model used for the multipath simulation takes both code and phase multipath into account. The code multipath simulation assumes so-called narrow-sampling and no fractional phase shift as described in [Byun et al., 2002], [Leick, 2004], [Joosten and Irsigler, 2003]. The following expressions are used for the multipath simulations of the code multipath error $\Delta\tau_c$ and the phase multipath error $\Delta\tau_\phi$:

$$\Delta\tau_c(i) = \begin{cases} \frac{\Delta\tau(i)\alpha \cos(\theta(i))}{1 + \Delta\tau(i)\alpha \cos(\theta(i))} & \text{if } \Delta\tau(i) < T_c - I + \Delta\tau_c(i) \\ I\alpha \cos(\theta(i)) & \text{if } T - I + \Delta\tau_c(i) < \Delta\tau(i) < I + \Delta\tau_c(i) \\ \frac{(T_c + I - \Delta\tau(i))\alpha \cos(\theta(i))}{2 - \Delta\tau(i)\alpha \cos(\theta(i))} & \text{if } I + \Delta\tau_c(i) < \Delta\tau(i) < T_c + I + \Delta\tau_c(i) \\ 0 & \text{if } \Delta\tau(i) > T_c + I + \Delta\tau_c(i) \end{cases} \quad (10)$$

$$\Delta\tau_\phi(i) = \arctan\left(\frac{\alpha A(i) \sin(\theta(i))}{1 + \alpha A(i) \cos(\theta(i))}\right)$$

with α the attenuation of the reflected signal path, $\theta(i)$ the multipath phase shift at epoch i , T_c the chip length of the code signal in seconds, I the sampling interval of the correlator, $\tau(i)$ the time delay of the reflected signal, and $A(i)$ the code correlation function. The code correlation function is sufficiently approximated [Parkinson and Spilker, 1996] by:

$$A(i) = 1 - \frac{|\Delta\tau(i)|}{T_c} \quad (11)$$

The multipath phase shift $\theta(i)$ is obtained as follows:

$$\theta(i) = \frac{2\pi}{\lambda_j} PD(i) = 2\pi f_j \Delta\tau(i) \quad (12)$$

With $PD(i)$ the path delay that can be obtained, see figure 5, by:

$$PD = S'R - SR \quad (13)$$

3.3.2 Multipath scenario

In the simulations for our measurement scenario we have assumed a vertical reflector at an azimuth of 1.45π with was placed at respectively a distance d of 1 meter, 30 meter and 50 meter. Three values for the attenuation were simulated from very strong reflection ($\alpha=0.9$), to moderate ($\alpha=0.5$) to weak reflections ($\alpha=0.1$), Byun et al. [2002] and Leick [2004] used $\alpha=0.1$ in their contributions. For the C/A code a chip length of 977 ns was used, with a sampling interval of 49 ns. The P2 code chip length was set at 98 ns and a sampling interval has been chosen of 65 ns. Figure 6 show the length of the delayed path for the two satellites and the different distances of the reflecting surface to the receiver.

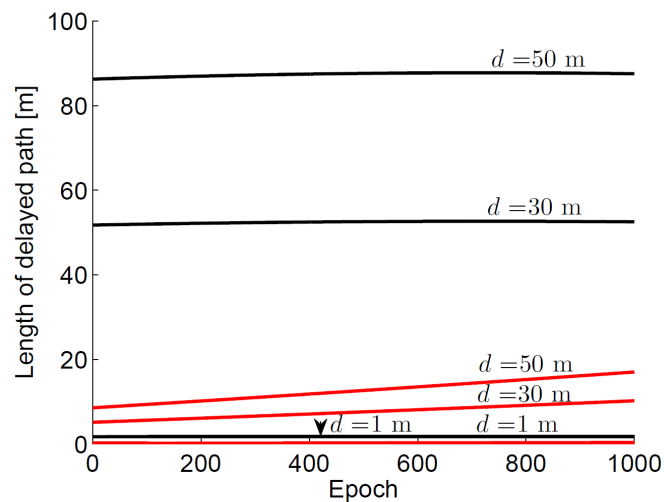


Figure 6: Length of the delayed path for PRN3 (red) and PRN31 (black) for different distance d of the reflecting vertical plane

For PRN3 the length of the delayed path increases slowly during the experiment. The delayed path of PRN31 is varying less for the duration of the experiment, but is larger than the delayed path of PRN3. The resulting influence of the multipath on the code and phase observations is shown in figure 7 for the $L1$ frequency and for the $L2$ frequency in figure 8.

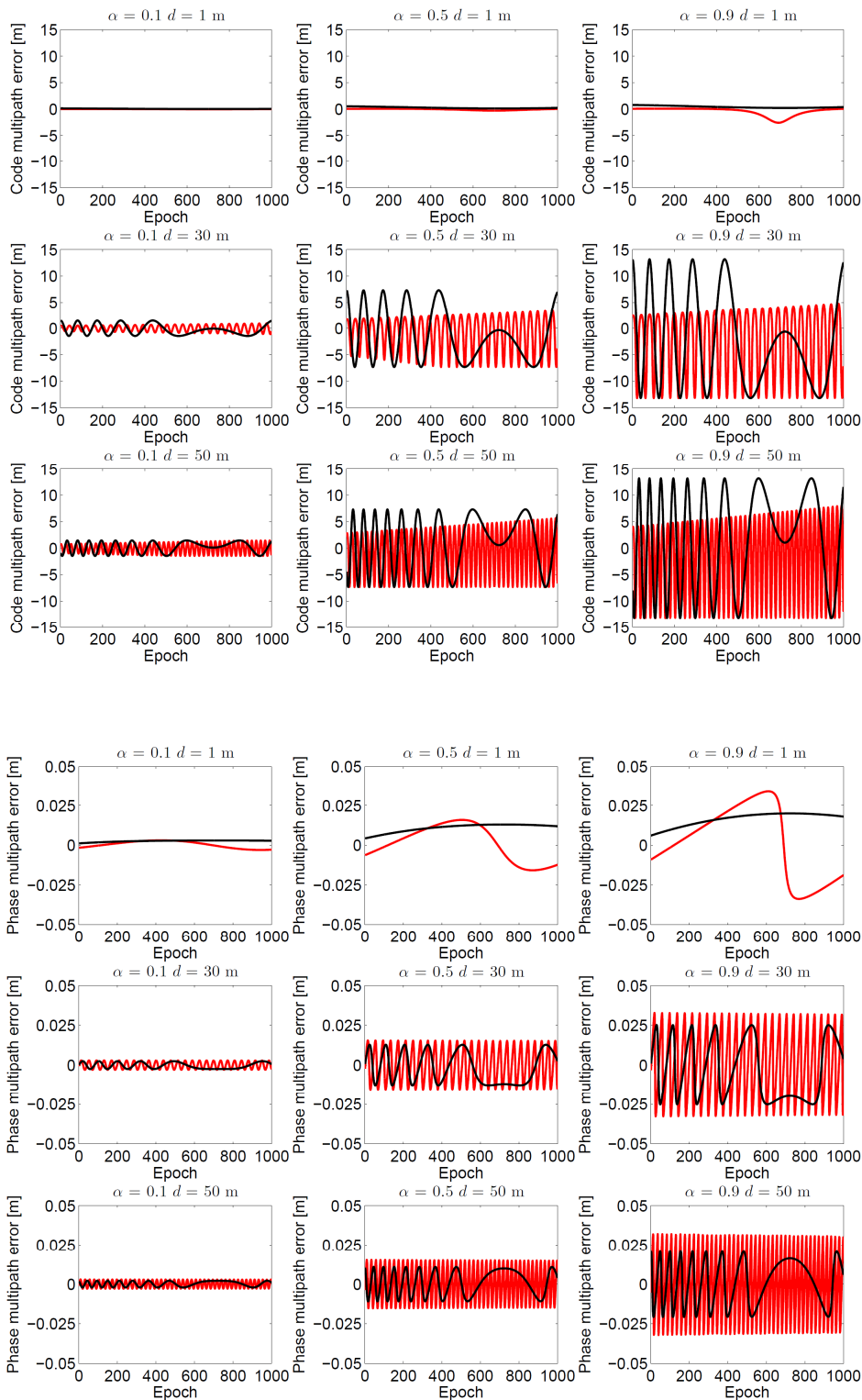


Figure 7: CA-code (top) and L1-phase (bottom) multipath error for PRN3 (red) and PRN31 (black) in the simulated scenarios

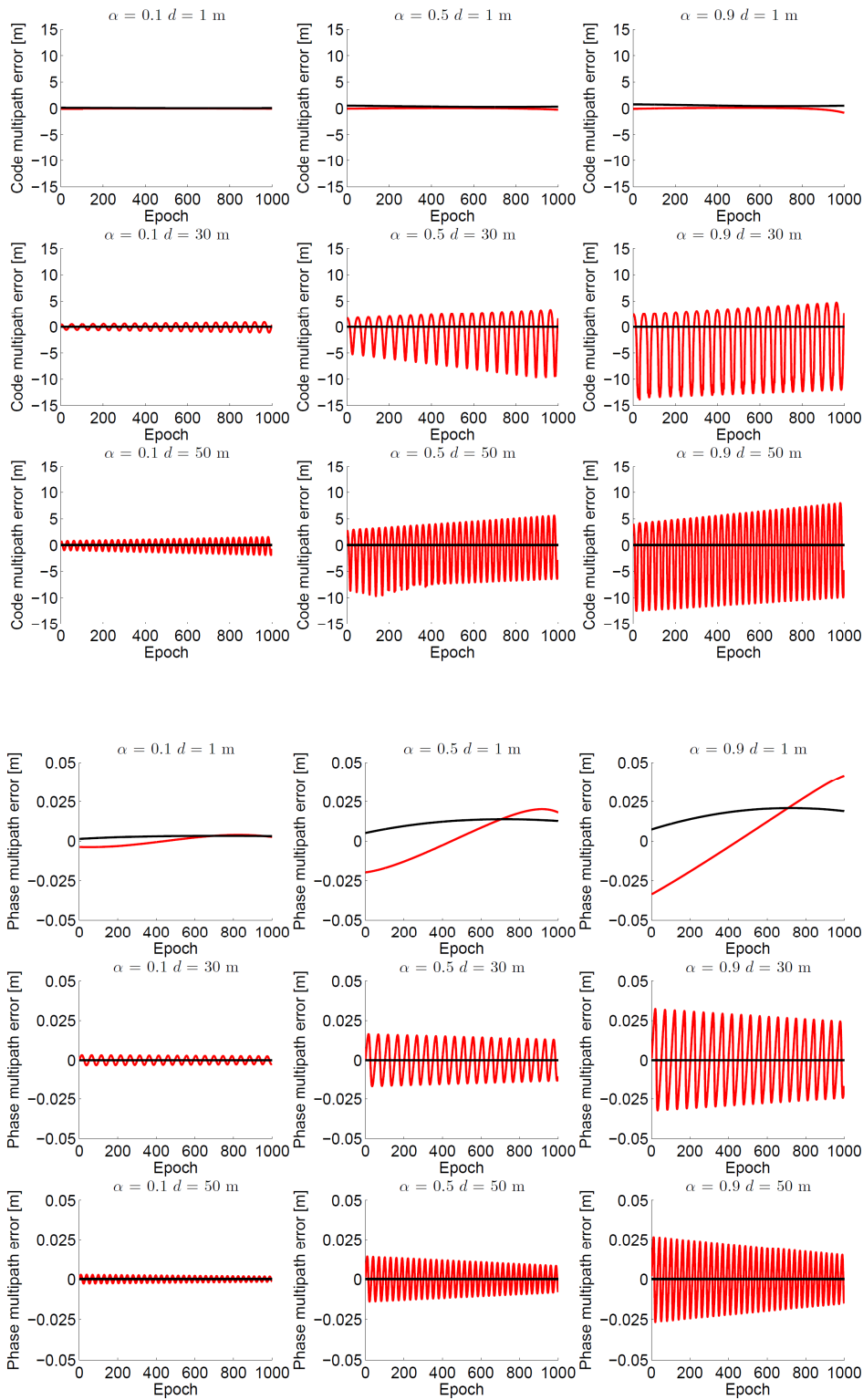


Figure 8: P2-code (top) and L2-phase (bottom) multipath error for PRN3 (red) and PRN31 (black) in the simulated scenarios

The effect of multipath on the $P2$ code observations is smaller than the code multipath error on the C/A code observations. The $L1$ and $L2$ errors are of the same magnitude.

3.3.3 Experimental results

Table 4 shows the empirical success-rates for dual-epoch processing for phase-only ($L1/L2$) observables and phase+code observables ($C/A/L1/P2/L2$). The empirical success-rates without multipath are 0.9980 for phase-only and 1.0000 for phase+code.

α	$d[m]$	observables $L1/L2$	observables $C\backslash A/L1/P2/L2$
0.1	1	0.998	0.885
	30	0.998	0.552
	50	0.998	0.524
0.5	1	0.683	0.489
	30	0.811	0.552
	50	0.846	0.528
0.9	1	0.259	0.472
	30	0.422	0.518
	50	0.530	0.500

Table 4: The empirical phase-only dual-epoch success-rate

The table clearly shows the degradation of the empirical success-rates in the presence of code multipath. Even without hardly any code multipath in the case of a distance of the vertical plane of 1 meter and $\alpha=0.1$ (see figures 7 and 8 for the size of the corresponding multipath errors) the success-rate of the code+phase solutions are lower than that of the phase-only processing. With low reflection values ($\alpha=0.1$) the ambiguity resolution of the phase-only processing is almost insensitive for the multipath errors, where the performances of phase-only and code+phase are comparable in strong multipath conditions ($\alpha=0.9$).

From (3 iii) it is clear that the 'fixed' baseline coordinates do not only rely on the integer ambiguities but also depend on the 'float' baseline coordinates. In case of correctly solved ambiguities the 'fixed' solution can still be biased due to a large bias in the 'float' solution. Therefore we also looked at the number of correctly fixed baseline components in case the ambiguities were fixed correctly. The criterion used for identifying a correct solution of the fixed baseline is an error smaller than 1 centimeter in the horizontal components and smaller than 2 centimeter in the vertical component. The benchmark values for the baseline length and height difference between the two receivers are obtained with a Sokkia Set1X total station. These measurements give us reference values for the observed baseline with a precision of 1 millimeter. Table 5 gives the ratio between the number of epochs with correct baseline solutions and the number of epochs with correctly fixed ambiguities.

The table shows that if the ambiguities are resolved correctly in case of phase-only processing it is likely that the fixed baseline components are also correct. The fixed baseline coordinates in case of code and phase dual-epoch processing are heavily influenced by the multipath errors on the code observations and are generally wrong. This shows that fixing the correct ambiguities does not necessarily give the correct solution for the other unknowns.

α	$d[m]$	<i>observables</i> L1/L2	<i>observables</i> C\A/L1/P2/L2
0.1	1	1.000	0.000
	30	1.000	0.103
	50	1.000	0.095
0.5	1	0.991	0.000
	30	0.995	0.111
	50	0.998	0.129
0.9	1	0.958	0.000
	30	0.924	0.139
	50	0.981	0.116

Table 5: The ratio between correctly fixed baseline components and correctly fixed integer ambiguities

4. CONCLUSIONS

In this contribution we studied the epoch-by-epoch or single-epoch RTK-capability of the short-baseline GNSS phase-only model, both in the absence and the presence of multipath. The performance of short-baseline, phase-only integer ambiguity resolution was shown for varying measurement precision, varying observation intervals and for single-, dual- and triple-frequency data varying the number of tracked satellites. Although single-epoch, phase-only ambiguity resolution is impossible, it becomes possible in the dual- and triple-frequency cases when six, respectively, five satellites are tracked.

It was also shown that the phase-only RTK model is more robust against multipath than the standard phase+code RTK model. In particular for attenuations up to $\alpha=0.5$, the phase-only success-rates are significantly larger than those of phase+code. Furthermore it was shown that in case of correct ambiguity resolution, the phase-only fixed baselines are more reliable than their phase+code counterparts.

ACKNOWLEDGMENTS

Professor P.J.G. Teunissen is the recipient of an Australian Research Council Federation Fellowship (project number FF0883188): this support is greatly acknowledged.

REFERENCES

- Byun, S.H., G.A. Hajj and L.E. Young (2002): *Development and application of GPS signal multipath simulator*, Radio Science, 37, 1-23.
- de Jonge P.J., C.C.J.M. Tiberius (1996): *The LAMBDA method for integer ambiguity estimation: implementation aspects*. Publications of the Delft Computing Centre, LGR-Series No. 12.
- Hofmann-Wellenhof, B., H. Lichtenegger, E. Wasle (2008): *GNSS: Global Navigation Satellite Systems, GPS, GLONASS, Galileo and more*. Springer Verlag.
- Joosten, P., M. Irsigler (2003): *GNSS ambiguity resolution in the presence of multipath*. *Proceedings European Navigation Conference 2003*, 15 p.
- Leick, A. (2004): *GPS Satellite Surveying*. 3rd edition, John Wiley, New York.
- Misra, P., P. Enge (2006): *Global Positioning System: Signals, Measurement and Performance*. 2nd edition. Ganga-Jamuna Press.
- Parkinson, B., J.J. Spilker (eds) (1996): *GPS: Theory and Applications*, Vols 1 and 2, AIAA, Washington DC.
- Strang, G., K. Borre (1997): *Linear Algebra, Geodesy, and GPS*, Wellesley-Cambridge Press.
- Teunissen, P.J.G. (1995): *The least-squares ambiguity decorrelation adjustment: a method for fast GPS integer ambiguity estimation*. Journal of Geodesy, 70: 65-82.
- Teunissen, P.J.G. (1998): *Success probability of integer GPS rounding and bootstrapping*. Journal of Geodesy, 72, 606-612.
- Teunissen, P.J.G. (1999): *An optimality property of the integer least- squares estimator*. Journal of Geodesy, 73: 587-593.
- Teunissen, P.J.G., C.C.J.M. Tiberius, P.J. de Jonge (1997): *The least- squares ambiguity decorrelation adjustment: its performance on short GPS baselines and short observation spans*. Journal of Geodesy, 71:589-602.
- Teunissen, P.J.G., A. Kleusberg (eds) (1998): *GPS for Geodesy*, 2nd enlarged edition, Springer Verlag.
- Thomson, H.F. (2000): *Evaluation of upper and lower bounds on the success probability*. In: Proc. ION GPS-2000, Nashville, pp. 183- 188.

Tiberius, C.C.J.M., P.J. de Jonge (1995): *Fast positioning using the LAMBDA method*. Proceedings DSNS-95, paper 30, 8p.

Verhagen S (2003): *On the approximation of the integer least-squares success-rate: which lower or upper bound to use?* Journal of Global Positioning Systems, 2(2), 117-124.

CONTACT

Ir. Lennard Huisman
Spatial Sciences – GNSS Research Lab
Curtin University
GPO Box U1987, Perth, Western Australia, 6845
Tel. . +61 (8) 9266 3517
Email: L.Huisman@curtin.edu.au